

Optical Engineering

OpticalEngineering.SPIEDigitalLibrary.org

Modeling of a fiber-optic surface plasmon resonance biosensor employing phosphorene for sensing applications

M. Saifur Rahman
Md. Shamim Anower
Lway Faisal Abdulrazak
Md. Maksudur Rahman

SPIE.

M. Saifur Rahman, Md. Shamim Anower, Lway Faisal Abdulrazak, Md. Maksudur Rahman, "Modeling of a fiber-optic surface plasmon resonance biosensor employing phosphorene for sensing applications," *Opt. Eng.* **58**(3), 037103 (2019), doi: 10.1117/1.OE.58.3.037103.

Modeling of a fiber-optic surface plasmon resonance biosensor employing phosphorene for sensing applications

M. Saifur Rahman,^{a,*} Md. Shamim Anower,^a Lway Faisal Abdulrazak,^b and Md. Maksudur Rahman^c

^aRajshahi University of Engineering and Technology, Department of Electrical and Electronic Engineering, Rajshahi, Bangladesh

^bCihan University-Slemani, Department of Computer Science, Sulaimaniya, Iraq

^cBangladesh Army University of Science and Technology, Department of Electrical and Electronic Engineering, Saidpur, Bangladesh

Abstract. An enhanced optical fiber-based surface plasmon resonance (SPR) biosensor is proposed utilizing a two-dimensional phosphorene heterostructure as an interacting layer with the analyte. This is the first model so far of a phosphorene-based fiber-optic SPR biosensor. High sensitivity and figure of merit (FOM), the two desirable parameters, are analyzed to investigate sensor performance. The analysis indicates that the proposed sensor provides significantly higher sensitivity in comparison to conventional fiber-optic SPR sensors. Numerical study shows that on using 10 layers of phosphorene on the Ag layer, the fiber-optic biosensor exhibits extremely high sensitivity of 3725 nm/RIU with a FOM of 61 RIU⁻¹. FOM reaches its maximum value of 64 RIU⁻¹ with six layers of phosphorene. Effects of the number of heterostructure layers and light wavelength on sensitivity are also analyzed. The results will open a new way for using phosphorene heterostructure in an optical fiber-based SPR sensor for biosensing applications. © 2019 Society of Photo-Optical Instrumentation Engineers (SPIE) [DOI: 10.1117/1.OE.58.3.037103]

Keywords: phosphorene; sensitivity; figure of merit; surface plasmon resonance angle; transmittance.

Paper 181693 received Nov. 28, 2018; accepted for publication Feb. 27, 2019; published online Mar. 21, 2019.

1 Introduction

Surface plasmon resonance (SPR) sensors have become the most convenient sensors for biochemical materials, because preprocessing, such as fluorescence labeling, is not required and because real-time analysis is possible.¹ Though many materials have been used in the modeling of SPR-based sensors, the two-dimensional (2-D) nanomaterials have attracted great attention for the past few years. Because of their unique optical, electronic, and catalytic properties, 2-D nanomaterials have been used in biosensing applications.² Graphene is one of the most extensively used 2-D nanomaterials since its discovery by Novoselov et al.³ It is the thinnest and strongest transparent tunable semiconductor, is a good thermal conductor, and has some unique features, such as ultralow phase distortion, relative high nonlinearity, and large optical absorption.⁴ Graphene-based SPR sensors are selected for biosensing applications, such as detecting single-stranded DNA (ssDNA) or *Pseudomonas* bacteria, because graphene has a large surface-to-volume ratio suitable for making contact with analytes.⁵ Another reason is that a graphene surface can selectively detect aromatic compounds through pi-stacking force.⁶

Following the successful attempt with graphene, extensive efforts have recently been dedicated to research another 2-D material called phosphorene.⁷⁻¹⁶ First, phosphorene is the monolayer 2-D black phosphorus (BP) having features, such as thickness-dependent direct bandgap and extraordinary electro-optical and high carrier mobility.^{9,11} Unlike graphene, phosphorene is a semiconductor with an intrinsic band gap that can be modified in a range from ~0.3 to 2.0 eV by changing the number of atomic layers^{10,11} and/or

sustained strains of the structure.^{12,13} Moreover, stacking more atomic layers together has little influence on both Young's modulus and tensile strength.¹⁷ Owing to these interesting unique and superior features of phosphorene, it is predicted to be a strong competitor to graphene¹⁸ and is considered as a promising 2-D material.¹⁹ Thus, the prospects of incorporating phosphorene in nanoelectronic and nanophotonic technology have been readily envisioned.⁷⁻¹⁶ For example, recent studies⁷⁻⁹ have reported that black phosphorene is an appealing candidate for tunable photodetection, accessing a wide spectrum ranging from visible to infrared regime. Moreover, previous reports have also indicated that black phosphorene is an outstanding semiconductor material⁸⁻¹⁵ and a promising alternative electronic material to graphene, MoS₂, boron nitride, and so on, for transistor applications.⁹⁻¹² More recently, phosphorene is used in prism-based SPR biosensors and provides tremendous performance enhancement.^{20,21} Few-layer phosphorene results in 2.4 times²⁰ better sensitivity compared to conventional Ag-based SPR sensor and 105%²¹ better sensitivity compared to conventional Au-based SPR sensor.

Although few studies have investigated the prism-based SPR biosensors, the use of phosphorene in fiber-optic-based SPR biosensors is still untouched. The fiber-optic-based SPR sensors possess numerous advantages over prism-based SPR sensor.²² This paper numerically investigates the use of phosphorene in optical fiber-based SPR biosensor. DNA hybridization, because of its important role in the detection of >400 diseases, is considered as the target biomolecular interaction and an Ag-based fiber-optic SPR biosensor with additional BP layers is explored for this purpose. Also, the effect of phosphorene layers on the

*Address all correspondence to M. Saifur Rahman, E-mail: saifurrahman121042@gmail.com

performance parameters is analyzed and the selection of the optimized number of layers is reported in order to achieve high sensor performance. The performance of the proposed biosensor is evaluated in terms of sensitivity and figure of merit (FOM). Finally, a comparison on sensitivity is drawn with some recent fiber-optic SPR biosensors, which indicates the enhanced sensing capability of the proposed sensor. This paper is arranged as follows: Secs. 2 and 3 discuss the theoretical modeling of the sensor, including the schematic diagram and mathematical expressions of reflectivity, constituents, and performance parameters, as well as the results and discussions with the details of detection approach. Conclusions are provided in Sec. 4.

2 Theoretical Modeling of the Proposed SPR Sensor

2.1 Schematic Diagram of the Proposed Sensor

The proposed SPR biosensor scheme is composed of four layers, the configuration of which is shown in Fig. 1. This study is based on the wavelength interrogation method. The operating wavelength is taken to be 633 nm, considering the fact that the optical nonlinearity can be enriched at high frequency (low wavelength). For specifications of the optical fiber, a fiber core with a diameter of D (50 μm) and a sensing region L (5 mm) are taken where the cladding is removed. Ag film with a thickness of d_2 (40 nm) is provided to the uncladded portion of the fiber for making conventional SPR biosensor.²² In addition, another coating of phosphorene, which is the monolayer phosphorene,²¹ d_3 ($d_3 = N \times 0.53$ nm) is provided, where N is the number of phosphorene layers. Light is emitted with a wavelength of 633 nm from a polychromatic source and the corresponding data are collected using spectrometer and computer.

2.2 Mathematical Modeling for Reflectivity

Assuming that p -polarized light can generate surface plasma, whereas s -polarized light makes no contribution to SPR, p -polarized light is launched into one end of the fiber at the axial point, and arrives at the other end of the fiber such that dP is the power arriving at the other fiber end between the incident angles θ and $\theta + d\theta$; hence dP can be expressed as in Refs. 22 and 23:

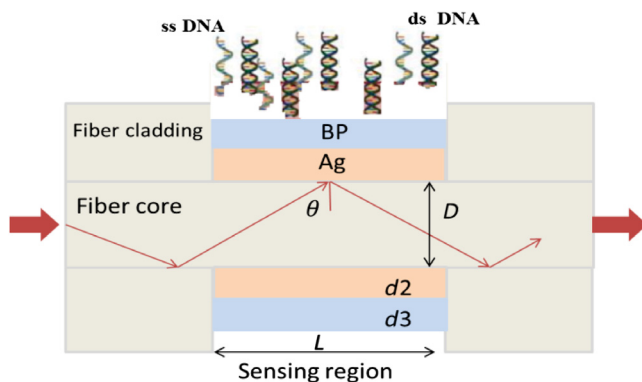


Fig. 1 Schematic diagram of the proposed phosphorene-based fiber-optic SPR biosensor.

$$dP \propto P(\theta) d\theta,$$

where $P(\theta)$ is the modal power relating to the incident angle θ and can be expressed as in Ref. 23:

$$P(\theta) = \frac{n_c^2 \sin \theta \cos \theta}{(1 - n_c^2 \cos^2 \theta)^2},$$

where n_c is the refractive index (RI) of the fiber core. Using the reflectance value, for a single reflection, as shown in Eq. (3), at the core/metal interface, the normalized transmitted power of the p -polarized light will be expressed as in Ref. 23:

$$P_{\text{trans}} = \frac{\int_{\theta_{cr}}^{\frac{\pi}{2}} R_p^{N_{\text{ref}}(\theta)} P(\theta) d\theta}{\int_{\theta_{cr}}^{\frac{\pi}{2}} P(\theta) d\theta}.$$

Here, $N_{\text{ref}}(\theta) = \frac{L}{D \tan \theta}$ is the total number of light reflections in the SPR fiber sensor by a ray. The incident angle of the ray is θ , with the normal to the core/metal layer interface in the sensing region. Here, L is the length of sensing region, d is the diameter of the fiber core, and θ_{cr} is the critical angle of the optical fiber [expressed as, $\theta_{cr} = \sin^{-1}(n_{cl}/n_c)$], and n_{cl} is the RI of the fiber cladding. The reflection R_p can be achieved by using the four-layer (fiber core, metal, BP, and sensing medium) model analysis.

The reflection intensity for the p -polarized light is expressed as in Ref. 24:

$$R_p = |r_p|^2, \quad (1)$$

where,

$$r_p = \frac{(M_{11} + M_{12}q_N)q_1 - (M_{21} + M_{22}q_N)}{(M_{11} + M_{12}q_N)q_1 + (M_{21} + M_{22}q_N)}, \quad (2)$$

$$M_{ij} = \left(\prod_{k=2}^{N-1} M_k \right)_{ij} = \begin{pmatrix} M_{11} & M_{12} \\ M_{21} & M_{22} \end{pmatrix}, \quad (3)$$

$$\text{with, } M_k = \begin{pmatrix} \cos \beta_k & -(i \sin \beta_k)/q_k \\ -iq_k \sin \beta_k & \cos \beta_k \end{pmatrix}, \quad (4)$$

$$\text{where, } q_k = \left(\frac{\mu_k}{\epsilon_k} \right)^{1/2} \cos \theta_k = \frac{(\epsilon_k - n_1^2 \sin^2 \theta_1)^{1/2}}{\epsilon_k}, \quad (5)$$

$$\beta_k = \frac{2\pi}{\lambda} n_k \cos \theta_k (z_k - z_{k-1}) = \frac{2\pi d_k}{\lambda} (\epsilon_k - n_1^2 \sin^2 \theta_1)^{1/2}. \quad (6)$$

2.3 Constituents of Sensor

2.3.1 Fiber core and cladding

For theoretical modeling, we have considered a step-index multimode fiber having silica core-doped GeO_2 (70%) to attain high core mode loss and pure silica as cladding. The wavelength-dependent RI (n_1) of the fiber core and cladding is given by the Sellmeier dispersion relation:²⁵

$$n_1(\lambda) = \left(1 + \frac{a_1 \lambda^2}{\lambda^2 - b_1^2} + \frac{a_2 \lambda^2}{\lambda^2 - b_2^2} + \frac{a_3 \lambda^2}{\lambda^2 - b_3^2} \right)^{1/2},$$

where $a_1, a_2, a_3, b_1, b_2,$ and b_3 are the Sellmeier coefficients. The values of Sellmeier coefficients are 0.6961663, 0.4079426, 0.8974794, 0.0684043×10^{-6} , 0.1162414×10^{-6} , and 9.896161×10^{-6} , respectively.²⁵

2.3.2 Metal layer

Silver has been considered an SPR active metal due to its low cost and lower values of the imaginary part of the RI with respect to gold. The lower value of the imaginary part of the RI is responsible for the lesser broadening of the SPR curve. For the dispersion relation in the metal layer, we invoke the Drude model, given in Ref. 26:

$$\epsilon_m(\lambda) = \epsilon_{mr} + \epsilon_{mi} = 1 - \frac{\lambda^2 \lambda_c}{\lambda_p^2 (\lambda_c + i\lambda)},$$

where λ_p and λ_c denote the plasma wavelength and collision wavelength, respectively. For silver, $\lambda_p = 1.4541 \times 10^{-7}$ m and $\lambda_c = 1.7614 \times 10^{-5}$ m.²⁶

The complex RI is taken from Ref. 23 at 633-nm incident wavelength and the value is $n_3 = 3.5 + (0.1)i$.²³ The fourth layer is the sensing medium, with a RI $n_s = 1.33$ (water).

2.3.3 Performance parameters of the proposed SPR Sensor

The main performance parameters of the SPR sensor are characterized based on its sensitivity, detection accuracy, and the quality factor; all these characteristics should be as high as possible for a good sensor.²⁷ The sensitivity, S , is defined as the ratio of a shift in the SPR wavelength ($\Delta\lambda_{\text{SPR}}$) to the RI change in the sensing region (Δn_a), and the dimension of sensitivity is measured in nanometer/refractive index unit:

$$S = \frac{\Delta\lambda_{\text{SPR}}}{\Delta n_a}. \quad (7)$$

FOM of the proposed sensor depends on the sensitivity and the spectral width of the SPR curve and is given as

$$\text{FOM} = S/\Delta\lambda_{0.5}(\text{RIU}^{-1}), \quad (8)$$

where $\Delta\lambda_{0.5}$ is the spectral width of the SPR curve corresponding to 50% reflectivity.²⁸

3 Performance Analysis

The following equation signifies the coupling of the incident light and SPs at the metal/dielectric interface:⁵

$$\frac{2\pi}{\lambda} n_p \sin \theta = \frac{2\pi}{\lambda} \sqrt{\frac{\epsilon_m \epsilon_s}{\epsilon_m + \epsilon_s}},$$

where n_p is the RI of the substrate medium (core), λ is the light wavelength, and ϵ_m and ϵ_s are the dielectric constants of the metal layer and the sensing (analyte) layer, respectively. Wavelength at which SPR curve dip (R_{min}) is obtained is termed as resonance wavelength. There is a shift in SPR dip with a change in analyte's RI. The resonance condition is very sensitive toward the RI variation of the surrounding sensing medium. Figure 2 shows the transmittance versus wavelength for sensing applications. As the RI of the sensing medium varies from 1.33 for water to 1.37 for sensing

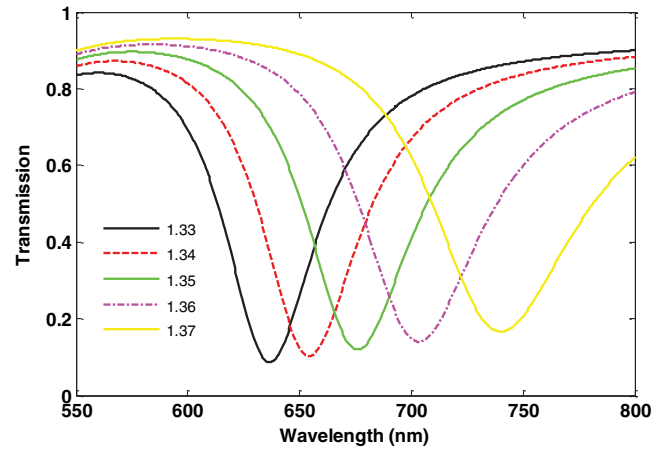


Fig. 2 The transmittance versus wavelength for different RIs.

applications, the corresponding SPR curves shift to higher resonance wavelength and their width becomes broader.

The SPR curve (red line) of the conventional ($N = 0$) SPR-based sensor is shown in Fig. 3(a). This performance characteristic is the base for our comparative study. The basic structure provides sensitivity of 2450 nm/RIU and its corresponding FOM value is 47 RIU^{-1} . To enhance the sensitivity of the SPR biosensor, a configuration based on the phosphorene is proposed where layers of phosphorene is applied over the Ag layer. Figure 3(a) demonstrates the SPR curves when N layer of phosphorene is coated on the Ag surface. The values $N = 1$ to 10 are chosen because of the experimental data.²⁹

As shown in Fig. 3(b), performance is enhanced with the addition of the number of BP layers. When one layer of BP is added, then sensitivity and FOM reach 2600 nm/RIU and 57 RIU^{-1} , respectively. And, in the case of the addition of two layers of BP, these performance parameters rise to 2650 nm/RIU and 58.25 RIU^{-1} , respectively. With this increment, the result in Fig. 3(b) shows that a sensitivity as high as 3725 nm/RIU can be obtained by applying 10 layers of phosphorene. So, a huge enhancement in sensitivity occurs in this case. Although sensitivity increases up to 10 layers of the phosphorene, it is not so for the FOM. It is clear from Fig. 3(c) that the FOM increases up to 64 RIU^{-1} for six layers, and then it decreases a little for the last four layers. Finally, Table 1 shows the comparison of the performance of the proposed phosphorene-based SPR sensor with other existing sensors in the literature,^{23,30,31} taking into account the sensitivity, enhancement strategy, and operating wavelength.

DNA hybridization detection approach is studied and discussed using MATLAB. This detection concept shows the transmittance-wavelength characteristic of the SPR-based DNA sensor before adding any DNA molecule (bare sensor), as shown in Fig. 4. In our calculations, the dependency of transmittance on wavelength is measured within the water. We first present how the RI changes with the change in concentration, and this relation can be expressed, as shown in Ref. 22, which is $n_a = n_s + c_a dn/dc$, where c_a is the concentration of adsorbed molecules, n_s is the RI of water, and dn/dc is the increment in RI due to the adsorbate. The RI increment parameter is $dn/dc = 0.182 \text{ cm}^3/\text{gm}$ when using a standard buffer solution.^{22,28,32} DNA molecules shift the SPR wavelength rightward due to the addition of a probe

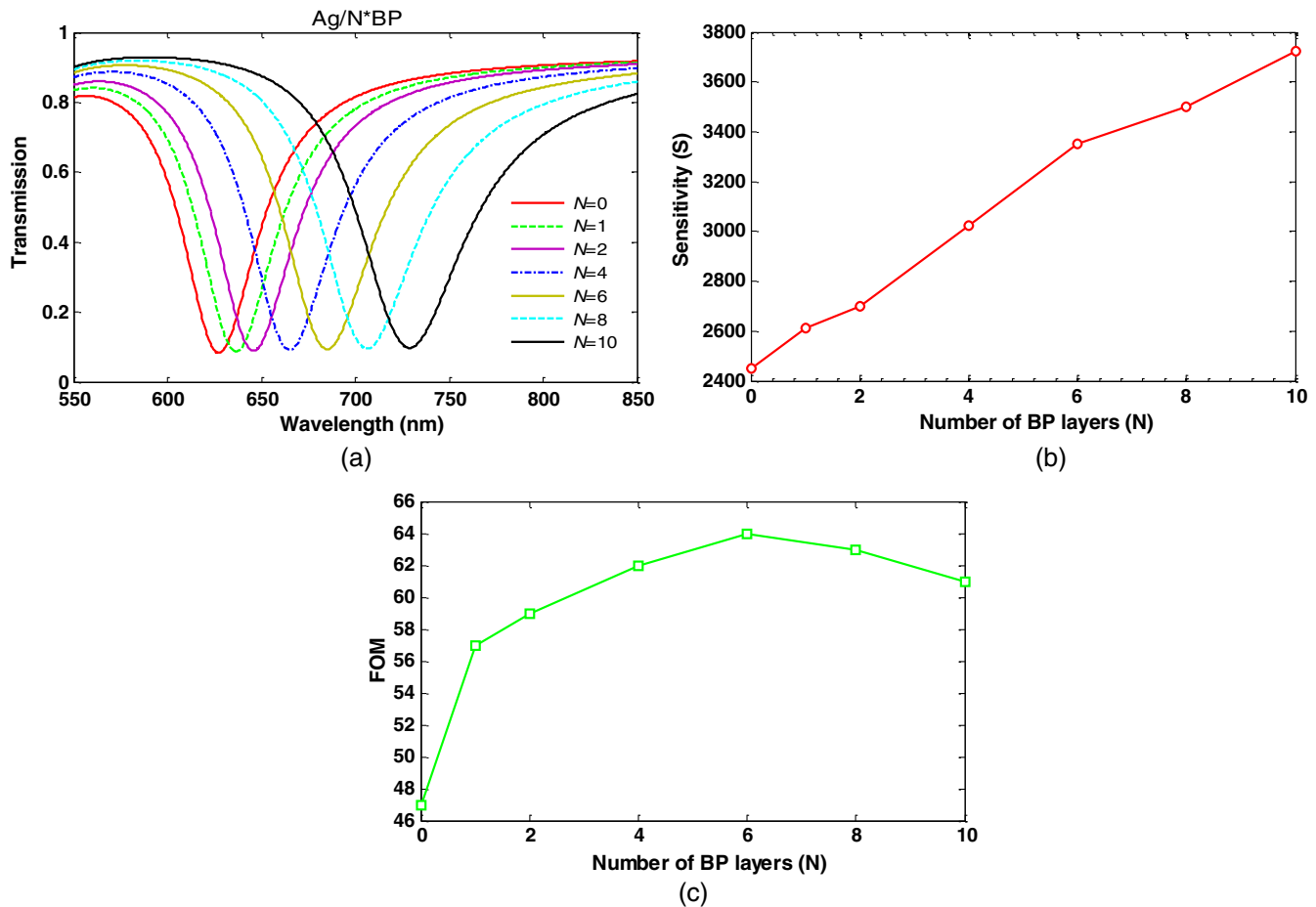


Fig. 3 (a) The transmittance variations as the function of the wavelength for different number of phosphorene layers over the Ag film, (b) sensitivity of the biosensor with respect to the number of phosphorene layers on the silver surface, and (c) FOM of the biosensor with respect to the number of phosphorene layers on the silver surface.

Table 1 Comparison of the proposed sensor with other existing sensors.

Ref.	Enhancement strategy	Wavelength (nm)	S (nm/RIU)
30	Au coating	633	2500
23	Au-graphene coating	633	2550
31	Au-graphene-MoS ₂ coating	633	3100
Proposed work	Ag-phosphorene coating	633	3725

which changes the RI of the sensing dielectric. By the introduction of DNAs as electron-rich molecules, the number of carriers changes in the layer concentration, which leads to a variation in the propagation constant. Thus, the proposed SPR sensor with high performance is applied to detect DNA hybridization based on the SP wavelength variations. As an example, we simulated the proposed SPR biosensor for the detection of the single-stranded DNA (ssDNA) in order to find out its numerical sensitivity. We initiated an assessment of the performance of the proposed sensor in terms of DNA hybridization detection by finding its SPR curves.

SPR curves with and without probe ssDNA, with single-base mismatch target ssDNA, and with complementary target ssDNA were obtained and are depicted in Fig. 4.

Figure 4 shows the transmittance versus wavelength curve with and without the DNA molecules. The wavelength in bare sensor is 636 nm (black line) and the wavelength while 1000 nM probe ssDNA is placed as sensing dielectrics is 646 nm (green line). The blue line shows the SPR curve with single-base mismatch ssDNA having 1000 nM concentration and provides 646.05 nm wavelength. Result shows no significant change in SPR wavelengths (change of SPR wavelength is 0.05 nm) of probe DNA and mismatch DNA. When the probe molecules is brought to the mismatched target, no hydrogen bonding takes place between the probe and target DNA strands because of the presence of mismatched base pair.³² So there is no significant change of charges in the target molecule. The red line demonstrates the final stage of detection concept when 1000 nM complementary ssDNA molecules are sunk in the probe. Result shows a significant change in the SPR wavelength (15 nm), due to the fact that the hydrogen bonding takes place between the probe and the target DNA strands because of the presence of matched base pair.³² So there is a considerable change of charges in the target molecule. Thus, DNA hybridization is easily detectable using the proposed phosphorene-based fiber-optic biosensor.

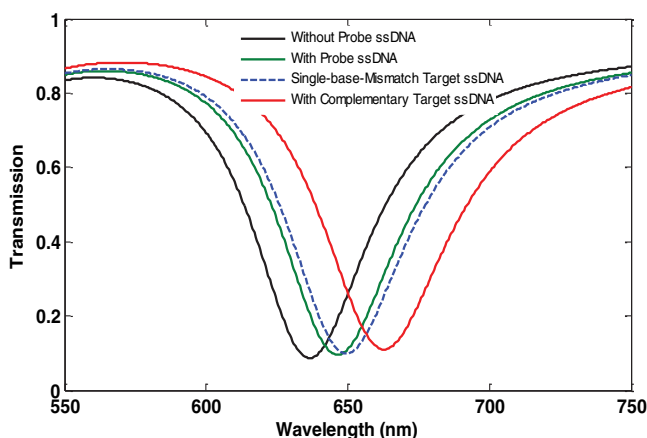


Fig. 4 The transmittance versus wavelength characteristics of the proposed sensor for sensing DNA hybridization.

4 Conclusion

The aim of the present effort was to investigate the use of phosphorene in fiber-optic SPR biosensors. A highly sensitive phosphorene-based fiber-optic SPR biosensor was numerically investigated to efficiently detect the DNA hybridization. The proposed structure exhibited improved sensitivity of 3725 nm/RIU by the addition of 10 layers of phosphorene between Ag and analyte. The sensitivity of the designed SPR sensor, with about 5 nm phosphorene sensing layer, was improved by 20%, 46%, and 49% than^{31,23,30} those without any phosphorene. Moreover, another performance parameter, i.e., FOM made up 64 RIU⁻¹ (36% increase) using only six phosphorene layers. Owing to its regular structure, the proposed biosensor can be realized using the existing fabrication technologies. This highly sensitive biosensor can be used for DNA hybridization detection, medical diagnostics, enzyme detection, food safety, and environmental monitoring.

References

1. J. Homola, "Present and future of surface plasmon resonance biosensors," *Anal. Bioanal. Chem.* **377**, 528–539 (2003).
2. C. Zhu et al., "Single-layer MoS₂-based nanoprobe for homogeneous detection of biomolecules," *J. Am. Chem. Soc.* **135**, 5998–6001 (2013).
3. K. S. Novoselov et al., "Electric field effect in atomically thin carbon films," *Science* **306**, 666–669 (2004).
4. A. Hoggard et al., "Using the plasmon linewidth to calculate the time and efficiency of electron transfer between gold nanorods and graphene," *ACS Nano* **7**, 11209–11217 (2013).
5. A. K. Sharma and A. K. Pandey, "Blue phosphorene/MoS₂ heterostructure based SPR sensor with enhanced sensitivity," *IEEE Photonics Technol. Lett.* **30**, 595–598 (2018).
6. G. B. McGaughey, M. Gagne, and A. K. Rappe, "Pi-stacking interaction-alive and well in proteins," *J. Biol. Chem.* **273**, 15458–15463 (1998).
7. F. Xia, H. Wang, and Y. Jia, "Rediscovering black phosphorus as an anisotropic layered material for optoelectronics and electronics," *Nat. Commun.* **5**, 4458 (2014).
8. J. Tao et al., "Mechanical and electrical anisotropy of few-layer black phosphorus," *ACS Nano* **9**, 11362–11370 (2015).
9. L. Li et al., "Black phosphorus field-effect transistors," *Nat. Nanotechnol.* **9**, 372–377 (2014).
10. V. Tran et al., "Layer-controlled band gap and anisotropic excitons in few-layer black phosphorus," *Phys. Rev. B* **89**, 235319 (2014).
11. N. Mo et al., "Anisotropy of black phosphorus in the visible regime," *J. Am. Chem. Soc.* **138**(1), 300–305 (2016).
12. H. Liu et al., "Phosphorene: an unexplored 2D semiconductor with a high hole mobility," *ACS Nano* **8**, 4033–4041 (2014).
13. T. Hu, Y. Han, and J. Dong, "Mechanical and electronic properties of monolayer and bilayer phosphorene under uniaxial and isotropic strains," *Nanotechnology* **25**, 455703 (2014).

14. H. Liu et al., "Semiconducting black phosphorus: synthesis, transport properties and electronic applications," *Chem. Soc. Rev.* **44**, 2732–2743 (2015).
15. J. Kang et al., "Probing out-of-plane charge transport in black phosphorus with graphene-contacted vertical field-effect transistor," *Nano Lett.* **16**, 2580–2585 (2016).
16. W. F. Li et al., "Ultrafast and directional diffusion of lithium in phosphorene for high-performance lithium-ion battery," *Nano Lett.* **15**, 1691–1697 (2015).
17. L. Li and J. Yang, "On mechanical behaviors of few-layer black phosphorus," *Sci. Rep.* **8**, 3227 (2018).
18. L. Li, Y. Yu, and G. Ye, "Electronic properties of few-layer black phosphorus," in *APS March Meeting* (2013).
19. H. O. Churchill and P. Jarillo-Herrero, "Two-dimensional crystals: phosphorus joins the family," *Nat. Nanotechnol.* **9**(5), 330–331 (2014).
20. L. Wu, J. Guo, and Q. Wang, "Sensitivity enhancement by using few-layer black phosphorus-graphene/TMDCs heterostructure in surface plasmon resonance biochemical sensor," *Sens. Actuators B Chem.* **249**, 542–548 (2017).
21. B. Meshginqalam and J. Barvestani, "Performance enhancement of SPR biosensor based on phosphorene and transition metal dichalcogenides for sensing DNA hybridization," *IEEE Sens. J.* **18**, 7537–7543 (2018).
22. M. S. Rahman et al., "Modeling of highly sensitive MoS₂-graphene hybrid based fiber optic SPR biosensor for sensing DNA hybridization," *Optik* **140**, 989–997 (2017).
23. K. N. Shushama et al., "Graphene coated fiber optic surface plasmon resonance biosensor for the DNA hybridization detection: simulation analysis," *Opt. Commun.* **383**, 186–190 (2017).
24. J. B. Maurya et al., "Performance of graphene-MoS₂ based surface plasmon resonance sensor using silicon layer," *Opt. Quantum Electron.* **47**, 3599–3611 (2015).
25. A. K. Ghatak and K. Thyagarajan, *Introduction to Fiber Optics*, Cambridge University, Cambridge (1998).
26. A. K. Sharma, R. Jha, and B. D. Gupta, "Influence of dopants on the performance of a fiber optic surface plasmon resonance sensor," *Opt. Commun.* **274**, 320–326 (2007).
27. A. Verma, A. Prakash, and R. Tripathi, "Sensitivity enhancement of surface plasmon resonance biosensor using graphene and air gap," *Opt. Commun.* **357**, 106–112 (2015).
28. M. S. Rahman et al., "Design and numerical analysis of highly sensitive Au-MoS₂-graphene based hybrid surface plasmon resonance biosensor," *Opt. Commun.* **396**, 36–43 (2017).
29. N. Mao, J. Tang, and L. Xie, "Optical anisotropy of black phosphorus in the visible regime," *J. Am. Chem. Soc.* **138**(1), 300–305 (2016).
30. Y. Wang et al., "Fiber-optic surface plasmon resonance sensor with multi-alternating metal layers for biological measurement," *Photonics Sens.* **3**(3), 202–207 (2013).
31. A. K. Mishra, S. K. Mishra, and R. K. Verma, "Graphene and beyond graphene MoS₂: a new window in surface-plasmon-resonance-based fiber optic sensing," *J. Phys. Chem. C* **120**(5), 2893–2900 (2016).
32. M. B. Hossain and M. M. Rana, "Graphene coated high sensitive surface plasmon resonance biosensor for sensing DNA hybridization," *ASP Sens. Lett.* **14**, 1–3 (2016).

M. Saifur Rahman is a student of BSc engineering in electrical and electronic engineering at Rajshahi University of Engineering and Technology (RUET), Rajshahi, Bangladesh. His current research interests include optical fibers and surface plasmon resonance biosensors.

Md. Shamim Anower received his BSc and MSc engineering degrees in electrical and electronic engineering from RUET. He obtained his PhD in electrical engineering from UNSW, Australia. Currently, he is working as a professor in the EEE Department, RUET. His current research interests include photonic crystal fibers, terahertz wave propagation, and surface plasmon resonance biosensors.

Lway Faisal Abdulrazak is currently working as a senior lecturer in the Department of Computer Science at Cihan University-Slemani, Sulaimaniya, Iraq. He got his PhD from University Technology Malaysia. His research interest includes network communication, antennas and propagation, and satellite communication.

Md. Maksudur Rahman is working as an assistant professor in the Department of EEE at Bangladesh Army University of Engineering and Technology. He got a BSc degree in electrical and electronic engineering from Chittagong University of Engineering and Technology, Bangladesh. His research interests include power electronics and optical devices.